Proceedings of the 5th World Congress on Mechanical, Chemical, and Material Engineering (MCM'19)
Lisbon, Portugal – August, 2019
Paper No. HTFF 118
DOI: 10.11159/htff19.118

Numerical Investigation on The Boundary Layer Development with the Effect of Wakes Generated by Translational Cascades

Xu Zhang[1], Pengfei Wang[2], Jiaming Wang[1], Xiaodong Ruan[1*], Zhongbin Xu[3] and Xin Fu[1]
[1]State Key Laboratory of Fluid Power and Mechatronic Systems, Zhejiang University
Hangzhou 310027, China
xdruan@zju.edu.cn
[2]School of Engineering, Zhejiang University City College
Hangzhou 310015, China
[3]Institute of Process Equipment, Zhejiang University
Hangzhou 310027, China

Abstract **-** In this paper, the boundary layer development with the effects of periodic wakes was investigated by numerical simulation. The accuracy of the numerical simulation is verified by experiments. The wake is generated by a prototype NACA0024 airfoil, and different length of flat plate (PL/D=0.88 and PL/D=4.8) was placed in the rear of airfoil. The results show that with the effects of periodic wakes, the pressure distributions on the flat plate surface with different length are similar, but the suction surface of the long flat plate is more likely to separate. In the view of vortex movement, the wake vortex moving along the pressure side of flat plate produces a reverse vortex due to the entrainment effects, and both the positive and negative vortex are continuously weakened due to viscous dissipation as they move to the end of the plate. It can be observed that the induced negative vortex was basically dissipated during 5/4 period for PL/D=4.8, and 1 period for PL/D=0.88. The vorticity in the boundary layer also shows some periodicities with the effects of wakes, but the vorticity distribution on the pressure surface shows a different tendency compared with the suction surface. Finally, the classical Time-Space (T-S) method was used to analyze the development of the boundary layer. It is found that the calmed region of the long flat plate is longer, which effectively suppresses the separation and pushes the transition point backward.

Keywords**:** Boundary layer, Wake, Vortex, T-S method.

1. Introduction

With over 60 years of extensive research, the development of compressor has reached a very high stage where improving the efficiency further has become progressively more difficult [1]. Compressors rely fundamentally on aerodynamic diffusion to achieve pressure rise, the unsteady interaction between rotating and stationary blade rows in compressors affects many aspects of performance such as blade loading, efficiency, heat transfer [2], stall margin and noise generation [3]. The adverse pressure gradient becomes strong at the high loading level, which would easily induce boundary layers to separate. Historically, the unsteady effects have been handled with semi-empirical approaches, i.e., the designers of compressors usually make use of the results of steady flow analysis obtained from experimental tests to design the blade profiles. However, such approaches simply establish design rules, they do not provide flow details and therefore cannot be used to optimize blade shapes. The current designers are looking for other ways reducing the number of blades or even the number of stages to save weight and acquire lower manufacturing and maintenance costs. As a result, the blade loading would increase and separation problems can be exacerbated if the adverse pressure gradient on the suction side become stronger [4], particularly under low Reynold number conditions [5]. The unattached boundary layer can deteriorate the aerodynamic performance and leads to efficiency decrease and loss increase [6].

Different from the natural boundary layer transition, the transition caused by the periodic passing of wakes from upstream rotating or stationary blade row is called wake-induced transition [4]. The wakes are a negative jet of fluid flowing toward the origin of the wake superimposed on a uniform freestream. These negative jets give rise to fluctuations in the surface velocity and pressure as they impinge on the suction surface of the blade. The wake-induced transition on the downstream blade surface is sensitive to many factors such as velocity deficit and turbulence of the incoming wakes. For low Reynold number compressor, both the wake's high turbulence and the negative jet behavior of the wake dominated the

interaction between the unsteady wake and the separated boundary layer on the suction surface of the blade, the separation can be suppressed as the wake strength increased [7].

The most representative works about boundary layer development are the research of Halstead [8]. They integrate the universal rules of boundary layer development in axial compressors and turbines. The effects of Reynold number, loading variation, wake frequency, turbulence intensity, and clocking are systematically evaluated. The Time-Space (T-S) analysis method proposed by them are widely used in recent research and the method was also used in this paper. Gete [9] found that the internal flow of compressor can be simplified by translational cascades and a fixed plate. Based on the experimental results of Gete, the wake-induced boundary layer transition was investigated using numerical simulation. The focus of this paper is to explore the effect of plate length on wake-induced boundary layer development.

2. Numerical Method

2.1. Geometry and Mesh

The experimental facility of Gete consists of two-dimensional translational airfoil cascades and a fixed flat plate at the back. The whole experiments were carried out in a wind tunnel with turbulence intensity=0.7%. The airfoil was fixed on a rotating belt to move vertically in front of the flat plate, thus the periodic passing of wakes reacts with the boundary layer of the flat plate. The detailed information about the experiment can be referred to the literature [9]. The airfoil used in the experiment is NACA0024 airfoil, the chord length is 50mm,

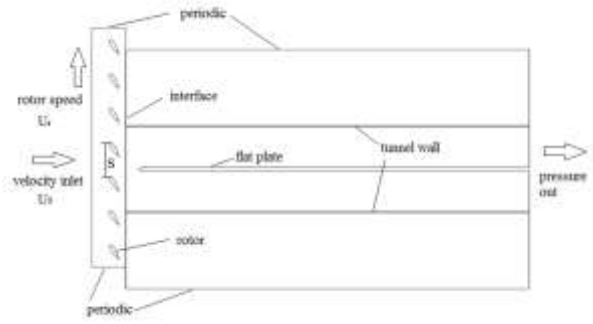

Fig. 1: Boundary conditions in the calculating domain.

the installation angle is 57.7 degree. The adjacent spacing between two airfoils is 100mm, the thickness of the flat plate is 12mm with a turbulence trigger wire installed at 20mm on the leading edge of the plate during the experiment. The distance between the leading edge of the flat plate and the trailing edge of the airfoil is 40mm. The unstructured grid was adopted for the entire domain to discrete the calculating zone. The grid element for airfoil cascades is 234512, and the grid element for the flat plate is 2236817, the total grid element is 2471329. Grid encryption is applied on the airfoil surface and the flat plate surface so as to ensure y^+=1 at the first layer of mesh. The calculation was performed with the commercial CFD code ANSYS Fluent 16.0.

2.2. Boundary Conditions and Numerical Setup

It is very important to apply correct boundary conditions in calculating domains for accurate and reliable results. According to the experimental setup, the velocity inlet is specified in the inlet with a fluid velocity U_0=3m/s, the outlet of the domain is specified with pressure outlet with the reference pressure=0 Pa. Both the airfoil wall and the flat plate wall are set to no-slip wall condition, the interface of the moving domain and the stationary domain is set to periodic repeats using sliding mesh. To keep similar to the compressor working conditions, the horizontal boundary of fluid domain is set to periodic boundary conditions. The specific boundary conditions are shown in Fig. 1.

The SST k-ω turbulence model is adopted in the calculation because the SST k-ω model has good prediction both in dealing with separate flow near the wall and free flow in the free streams [10]. The turbulence intensity of the wind

tunnel in the experiment is 0.7%, so a turbulence intensity=0.7% is also specified in the velocity inlet during the calculation. The discrete time step is 1×10^{-4}s for the unsteady calculation, which indicates that 333 time steps are calculated in a periodic cycle, and the convergence criterion is that the residual of calculated variables is less than 1×10^{-5}. The pressure based SIMPLE second order high-resolution discrete method is used to solve the unsteady case. Before the unsteady calculation is carried out, the steady calculation is performed and the steady results are specified to the initial condition for unsteady calculations. The unsteady calculation is statistically processed after the calculation has performed 20 periodic cycles.

2.3. Fonts

In order to ensure the accuracy and reliability of the calculation method, the grid independence verification is first carried out. The calculation results error of the current grid is less than 1% compared with the results of a denser grid, thus it proves that the current grid element is sufficient to resolve the flow field. On the other hand, the calculated results were compared with the experimental results obtained by Gete [9], the data used to compare is the boundary layer velocity profile with airfoil vertical velocity U_r=3m/s. From Fig. 2 it can be observed that the calculated results have good agreement with the experimental results, indicating that the current numerical method can accurately predict the velocity distribution of the boundary layer of the flat plate with the effects of periodic passing of wakes.

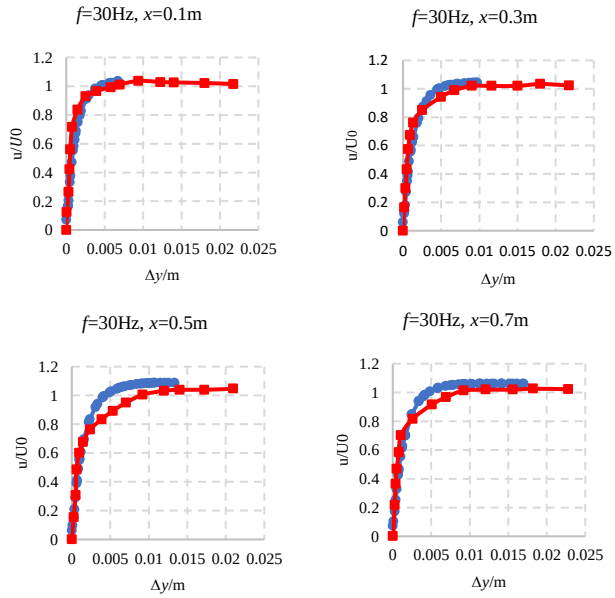

Fig. 2: Boundary layer velocity profiles-●-CFD -■-EXP.

3. Results and Analysis

3.1. Effects of Plate Length on Pressure Distribution

In order to investigate the effect of plate length on the development of boundary layer, let the airfoil and other parameters unchanged, the plate length of PL/D=0.88 and PL/D=4.8 are selected to for calculation. Firstly, the pressure distribution of the flat plate is presented in Fig.3. It can be observed that the pressure distribution of the leading edge is

almost the same for PL/D=0.88 and PL/D=4.8, the two curves are even partially overlapped, but the difference soon appeared, regardless of the suction side or the pressure side of the flat plate, the surface pressure of the long plate PL/D=4.8 was higher than that of the short plate PL/D=0.88. However, the surface pressure drop of the flat plate is not influenced by the length of plate. So, the lift of flat plate is free from the influence of plate length. Moreover, it can be observed that there

is no sudden pressure jump at the pressure side of the leading edge of short plate PL/D=0.88, by contrast, there is an obvious pressure jump at the pressure side of the leading edge of long plate PL/D=4.8. The pressure suddenly rose at *x*/D=1.26, indicating that the free shear layer turned to be transition flow, after the transition, the pressure value of pressure side rose rapidly and finally got to the same value of suction side. Regardless of the plate length, the pressure on both pressure side and suction side are the same after *x*/D=1.44, but the surface pressure of the long plate PL/D=4.8 is higher than that of the short plate *x*/D=0.88.

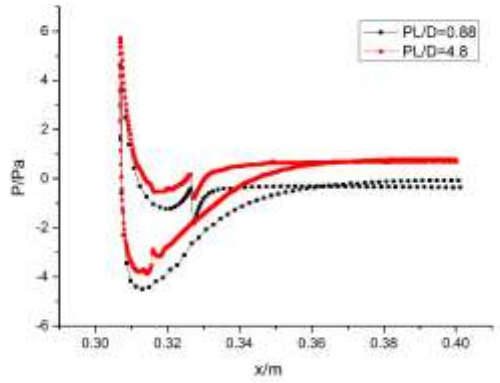

Fig. 3: Pressure distribution of long/short plat surface.

3.2. Vortex Evolution

The airflow passes through the airfoil and produced positive vortex on the pressure side and negative vortex on the suction side. And the vortex sheds from the trailing edge of airfoil forming a vortex street. Fig.4 showed the motion trace of the vortex generated by the airflow passing through the airfoils at different phases in a passing through period. *t'* represents different phases in a wake passing through period. It can be clearly observed that the vortex moving from the airfoil trailing edge to the suction side of the flat plate was cut off by the flat plate. Positive vortex exists on the pressure side of the plate, and negative vortex exists on the suction side of the plate. The positive vortex shedding from the trailing edge of airfoil is cut off by the plate and adhere to the suction side of the plate. Due to the viscous shear stress, the entrainment effect in the outer region of positive vortex P accelerates the outer layer of the adjacent negative vortex on the suction side of the plate. The accelerated rotation then induced a strong negative vortex N on the suction side.

Fig.4(c) is the enlarged view of the negative vortex pair induced by the positive vortex entrainment effect at PL/D=4.8. The high-speed positive vortex P1 swept along the suction side of the plate, and the strong shear of the positive vortex P1 forced the low-speed fluid in negative vortex N1 to accelerate and form a hairpin vortex, therefore the negative vortex N1 injected upward and induced a small-scale positive vortex P2 beneath the negative vortex N1.

Fig.5(c) is the enlarged view of the negative vortex pair induced by the positive vortex entrainment effect at PL/D=0.88. It can be observed that the vortex strength is weakened because of the high turbulence induced from the lack of flow rectification. The strength of the negative vortex P induced by entrainment effects was also weakened, and no further induced-vortex was observed in the wall. The positive vortex shedding from the pressure surface of airfoil moved parallel to the plate wall suction surface, its strength was steadily weakened due to the viscous dissipation, and the induced negative vortex on the suction surface was also weakened. It can be observed that the induced negative vortex was basically dissipated during 5/4 period for PL/D=4.8, on the contrast, the induced negative vortex was basically dissipated during 1 period for PL/D=0.88. the dissipating rate of induced negative vortex for PL/D=0.88 is higher than that of PL/D=4.8.

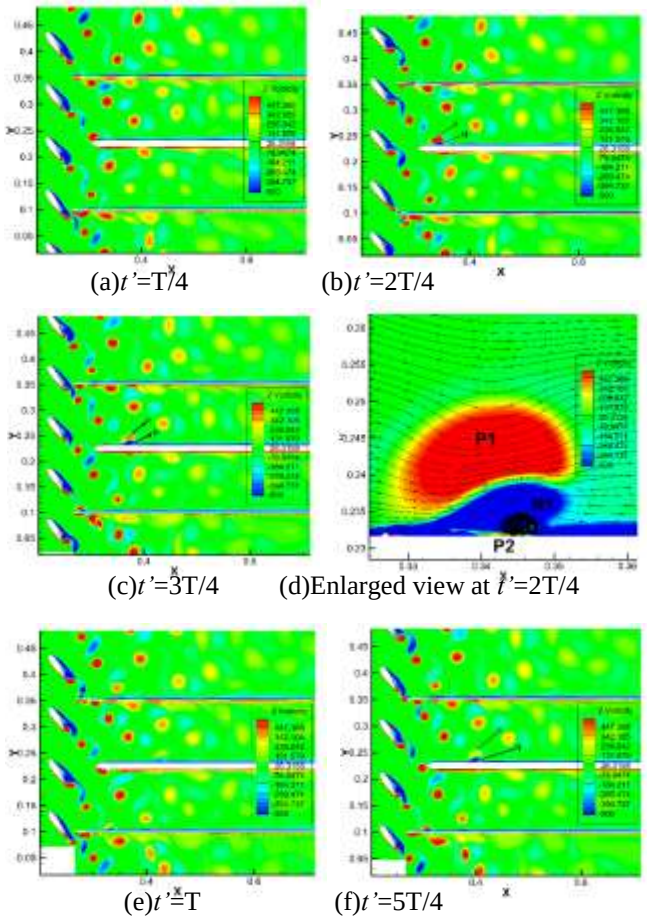

(a)t'=T/4 (b)t'=2T/4

(c)t'=3T/4 (d)Enlarged view at t'=2T/4

(e)t'=T (f)t'=5T/4

Fig. 4: Vortex evolution for PL/D=4.8.

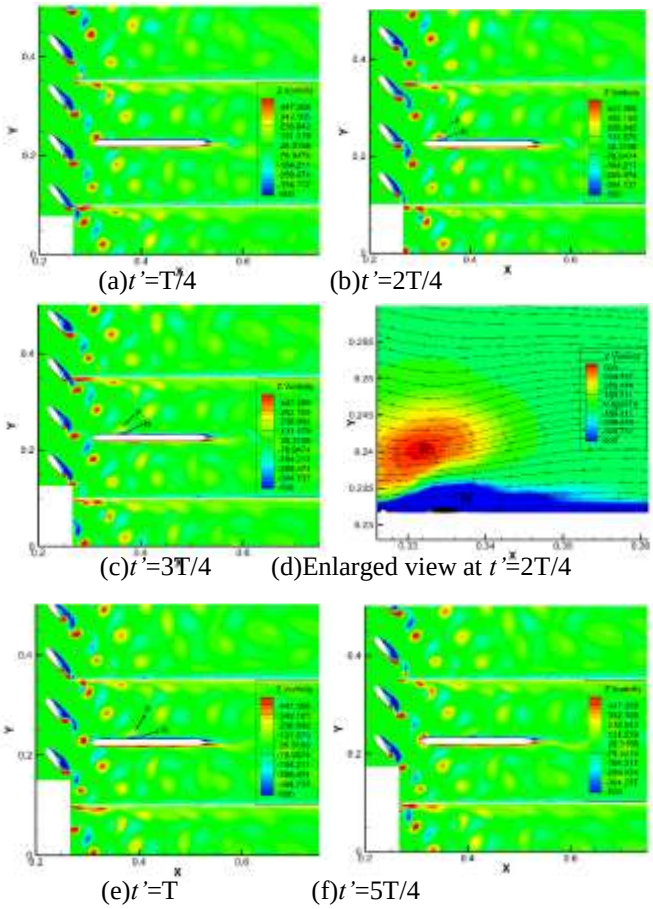

(a)t'=T/4 (b)t'=2T/4

(c)t'=3T/4 (d)Enlarged view at t'=2T/4

(e)t'=T (f)t'=5T/4

Fig. 5: Vortex evolution for PL/D=0.88.

3.3. Vorticity Pulsation

The moving trace of the wake in a passing period is shown in the previous section, the wake interacts with the boundary layer of the flat plate affecting the velocity pulsation in the boundary layer. In this section, the vorticity $\omega_z = \partial v/\partial x - \partial u/\partial y$ distributions at 2mm away from the pressure side and suction side are calculated.

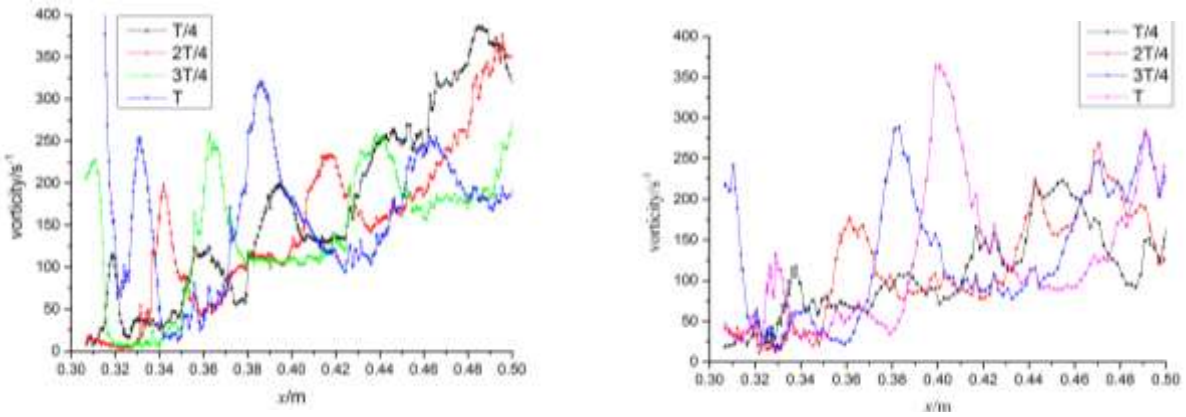

(a) Vorticity on suction side for PL/D=4.8. (b) Vorticity on suction side for PL/D=0.88.

Fig. 6: Boundary layer vorticity distribution on the suction side.

Fig. 6 shows the vorticity distribution on the suction surface of the flat plate. The vorticity distribution exists several peaks at a certain phase, the peak appears because there is a wake vortex in the peak location. As the vortex continuously sheds from the trailing edge of airfoil, there are several wake vortexes on the plate surface which induced several vorticity peaks in the boundary layer. Although the strength of the induced vortex on the suction surface is decreasing during the downstream movement, the vorticity in the boundary layer of the suction surface does not decrease during downstream flow, even shows a rising trend. The reason may be that the plate flow becomes a turbulent flow after the transition, the turbulence acts to increase the vorticity in the whole boundary layer. Regardless of the plate length, the vorticity on the suction surface has an increasing tendency in the flow direction.

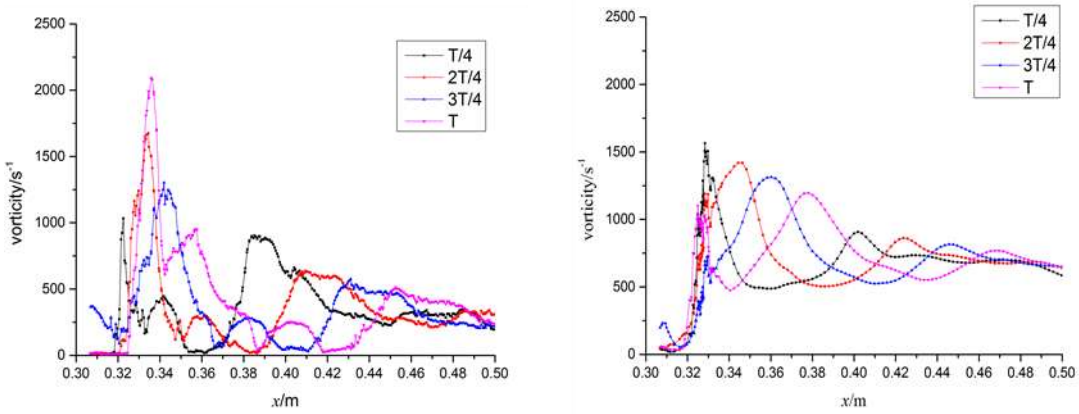

(a) Vorticity on pressure side for PL/D=4.8. (b) Vorticity on pressure side for PL/D=0.88.

Fig. 7: Boundary layer vorticity distribution on the pressure side.

The vorticity distribution on the pressure surface in Fig.7 shows a different tendency compared with the suction surface. The vorticity in the pressure side decreases in the flow direction, the vorticity in the leading edge of the flat plate is the largest because the wake vortex interacts with the boundary layer, the transition on the pressure surface is depressed so the turbulence contributes little to the vorticity. The vorticity decreases for two reasons: First, the wake vortex has vertical velocity in the plate flow, so the distance between wake vortex and pressure side boundary is progressively increases, the interaction of wakes is weakened because of distance increase. Second, the wake itself is dissipated by the viscous dissipation moving in the plate flow, the interaction of wakes is weakened because of wakes strength decline.

3.4. Space-Time Diagram of Turbulence Intensity

Halstead et al. [8] pointed out that the wake-induced boundary layer development of a compressor is affected by Reynold Reynold number, loading variation, wake frequency, turbulence intensity, and nozzle-nozzle interaction. In this paper, the the influence of plate length on boundary layer development is investigated. The space-time diagram is used to show the the wake-induced path in a manner analogous to that shown for the convecting (shaded) turbulent spot in Fig. 8.

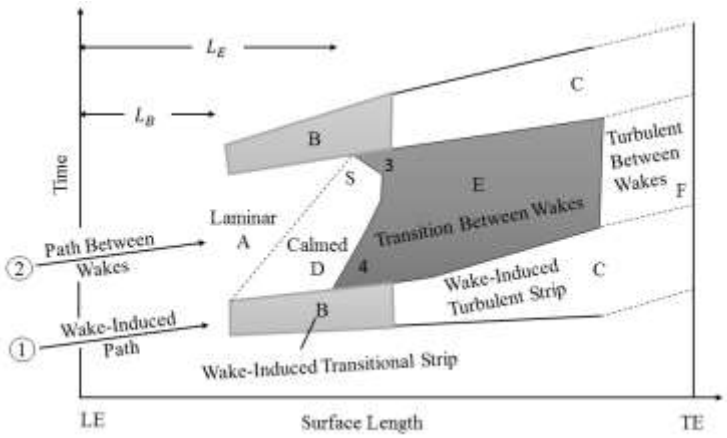

Fig. 8: Typical space-time diagram of a compressor [8].

The typical space-time diagram of compressor involved two separated but coupled paths mark as ① and ② in Fig.8 of wake-induced boundary layer development. The first path, shown as ① in Fig.8, called the wake-induced path, lies approximately under the wake trajectory but lags the wake for the compressor. The wake-induced path consists of the portion of laminar region A that lies under the wake trajectory, the wake-induced transitional strip B and wake-induced turbulent strip C. The second path, shown as ② in Fig.8, called the paths between wakes, follows the wake in time. It consists of the remaining laminar region A, the calmed region D, and the region of transition and turbulent flow between wakes labeled E and F, respectively.

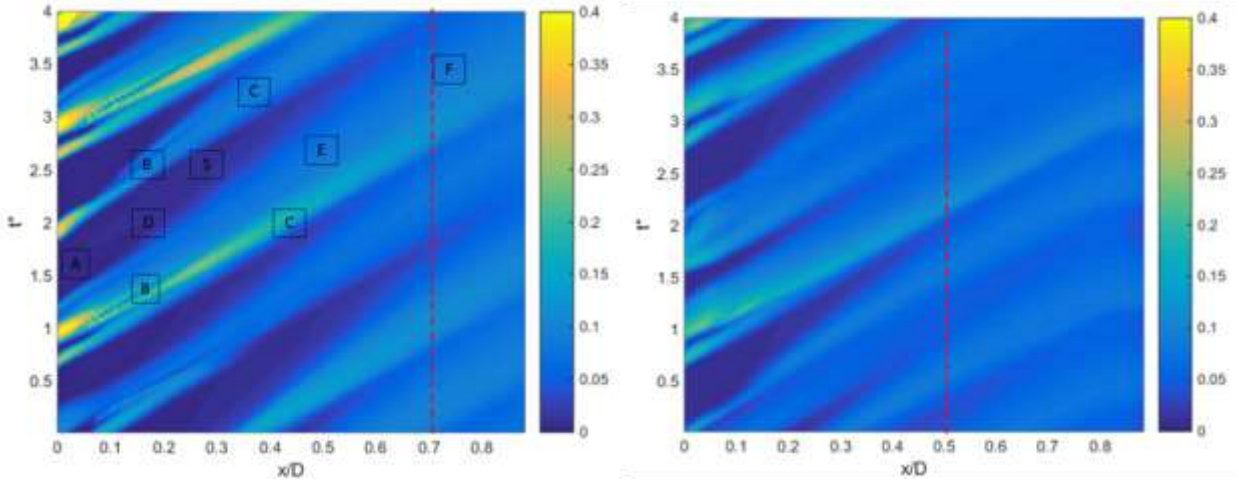

(a) PL/D=4.8. (b) PL/D=0.88.

Fig. 9: Space-time diagram of turbulence intensity.

Fig.9 shows the calculated space-time diagram of the turbulence intensity and the main regions are marked out in the figure. It can be seen that the calculation results are in good agreement with the classical theory. Generally, the laminar flow in path ① occupies only about 20 percent of the wake-passing period. It leads directly into the wake-induced transitional strip B. The transition does not happen directly at the leading edge of the blade, but some distance downstream marked as L_B in Fig.8, the distance length is related to the blade profile and its incidence angle. In this paper, the stationary blade is a flat plate, so the wake-induced transition happens directly at the leading edge of the flat plate. the wake-induced transitional flow occupied a considerable portion of the suction surface. Transition in these strips occurs via bypass mode. The transition strips are typically 20 percent of the wake-passing period. The wake-induced turbulence strips C that follow the region B extend to the trailing edge, and region C is similar for PL/D=4.8 and PL/D=0.88.

The calmed region D begins at the tail of the wake-induced transitional strip B and extends into the laminar region between wakes. Since calmed region D results from turbulent spot production and starts to grow after transition region B. it has effectiveness to suppress flow separation and determine the separation onset between wakes. The calmed region D disappeared across the wake-passing period as shear stress levels decay. S region, where the least calming region exists, is followed by boundary layer profile changing into inflectional and flow separation, in S region separation easily occurs when the operating condition changes slightly. As can be seen from Fig.8, the flow separation is suppressed by the calmed region, transition between wakes in region E occurs via the bypass mode. Comparing the calmed region of PL/D=4.8 with that of PL/D=0.88, it can be found that the calmed region on the suction surface of PL/D=4.8 is longer and extended to a position of about *x*/D=0.7, while the calmed region of PL/D=0.8 extends to a position of *x*/D=0.5. It shows that the flow separation is more likely to appear early when flat plate length is shortened.

4. Conclusion

In this paper, the reliability of the numerical method is verified by experimental results, and the boundary layer development and vortex evolution processes of long and short plates under wake effects are compared, the conclusions are as follows:

The pressure distributions of different plate length are similar, but there is a pressure jump on the leading edge of the pressure surface at PL/D=4.8, as a result, it is more likely to separate when increasing the plate length.

A negative vortex is induced by wake vortex on the suction side of the plate because of entrainment effects. The wake strength is weakened when plate length decreased. A positive vortex is induced beneath the wake-induced negative vortex for PL/D=4.8, but this phenomenon does not exist for PL/D=0.88. The dissipating rate of induced negative vortex for PL/D=0.88 is higher than that of PL/D=4.8.

The vorticity in the boundary layer shows some periodicities with the effects of wakes, but the vorticity distribution on the pressure surface shows a different tendency compared with the suction surface. The vorticity in the boundary layer is not only related to the wake effects but also related to the development of the boundary layer itself.

The calculated space-time diagram of turbulence intensity agrees well with the classical theory. The calmed region has an effect on suppressing transition and separation of the boundary layer, the flow separation is more likely to happen in advance when flat plate length is short. Therefore, for engineering application, appropriate lengthening of guide vane length can reduce the occurrence of flow separation.

Acknowledgements

This project is supported by the National Basic Research Program of China [Grant no. 2015CB057301], Zhejiang Provincial Natural Science Foundation of China [Grant no. LQ18E060002] and the Science Fund for Creative Research Groups of the National Natural Science Foundation of China [No. 51521064].

References

[1] R. J. Howell, O. N. Ramesh, H. P. Hodson, N. W. Harvey, V. V. Schulte, “High Lift and Aft-Loaded Profiles for Low-Pressure Turbines,” *ASME Journal of Turbomachinery*, vol. 123, no. 2, pp. 181-188, 2000.

[2] H. P. Hodson, “Boundary layer and loss measurements on the rotor of an axial-flow turbine,” *Journal of Engineering for Gas Turbines and Power*, vol. 106, no. 2, pp. 391-399, 1984.
[3] H. P. Hodson, “Measurements of Wake-Generated Unsteadiness in the Rotor Passages of Axial Flow Turbines,” *Journal of Engineering for Gas Turbines and Power*, vol. 107, no. 2, pp. 467-476, 1984.
[4] R. E. Mayle, “The Role of Laminar-Turbulent Transition in Gas Turbine Engines,” *ASME Journal of Turbomachinery*, vol. 113, no. 4, pp. 509-537, 1991.
[5] V. V. Schulte, H. P. Hodson, “Unsteady Wake-Induced Boundary Layer Transition in High Lift LP Turbines,” *ASME Journal of Turbomachinery*, vol. 120, no. 1, pp. 28-35, 1998.
[6] D. J. Dorney, P. King, J. P. Lake, D. Ashpis, “Experimental and Numerical Investigation of Losses in Low-Pressure Turbine Blade Rows,” *International Journal of Turbo and Jet Engines*, vol. 17, no. 4, pp. 241-254, 2000.
[7] L. Jia, T. Zou, Y. Zhu, T. Zou, C. Lee, “Rotor boundary layer development with inlet guide vane (IGV) wake impingement,” *Physics of Fluids*, vol. 30, no. 4, p. 040911, 2018.
[8] D. E. Halstead, D. C. Wisler, T. H. Okiishi, G. J. Walker, H. P. Hodson and H.-W. Shin, “Boundary layer development in axial compressors and turbines: Part 1 of 4—composite picture,” *ASME Journal of Turbomachinery*, vol. 119, no. 1, pp. 114-127, 1997.
[9] Z. Gete, R. L. Evans, “An experimental investigation of unsteady turbulent-wake/boundary-layer interaction,” *Journal of fluids and structures*, vol. 17, no. 1, pp. 43-55, 2003
[10] F. R. Menter, “Two-equation eddy-viscosity turbulence models for engineering applications,” *AIAA Journal*, vol. 32, no. 8, pp. 1598-1605, 1994.